Bioorganic & Medicinal Chemistry Letters 20 (2010) 5089–5094

Contents lists available at ScienceDirect

Bioorganic & Medicinal Chemistry Letters

journal homepage: www.elsevier.com/locate/bmcl

Inhibition of interleukin-1β converting enzyme (ICE or caspase 1) by aspartyl acyloxyalkyl ketones and aspartyl amidooxyalkyl ketones

Paul Galatsis [a,*], Bradley Caprathe [a], Dennis Downing [a], John Gilmore [a], William Harter [a], Sheryl Hays [a], Catherine Kostlan [a], Kristin Linn [a], Elizabeth Lunney [a], Kim Para [a], Anthony Thomas [a], Joseph Warmus [a], Hamish Allen [b], Kenneth Brady [b], Robert Talanian [b], Nigel Walker [b]

[a] Pfizer Global Research and Development, 2800 Plymouth Road, Ann Arbor, MI 48105, United States
[b] BASF Bioresearch Corporation, 100 Research Drive, Worcester, MA 01605, United States

ARTICLE INFO

Article history:
Received 26 March 2010
Revised 6 July 2010
Accepted 8 July 2010
Available online 11 July 2010

Keywords:
ICE inhibitor
Prime side
Hydrophobic pocket

ABSTRACT

A series of acyloxyalkyl and amidooxyalkyl ketones appended to a carbobenzyloxy aspartic acid core have been prepared. The most potent of these new inhibitors was **4i** with a K_i of 0.5 μM. These two series provide an improved understanding of the binding requirements for the hydrophobic prime side of ICE.

Interleukin IL-1β (IL-1β) is a pro-inflammatory cytokine that has been implicated in a number of pathophysiological states.[1] Thus inhibitors of ICE, the key enzyme that converts the inactive pro-IL-1β to the biologically active form, would be of pharmacological value.[2] Structurally, ICE inhibitors can be dissected into three components: a core fragment, a P4-P2 peptidomimetic head-fragment, and a prime side tail-fragment (Fig. 1). SAR campaigns buttressed by X-ray crystallography[3] have revealed a key requirement for Asp as the core fragment.[4] While multiple scaffolds have been disclosed for the peptidomimetic fragment, the prime side tail has received limited attention. Most of these moieties have been functionally designed as leaving groups, thus not taking full advantage of all the available protein interactions.

The simplest prime side group is the corresponding Asp-CHO, typically found in its masked acylal form, as exemplified by the clinical candidates pralnacasan[5] and VX-765[6] (Fig. 2). Other variations found for the prime side moiety include halomethyl Asp ketones (AcYVAD-CMK or MX-1122[7]), halophenyl derivatives (Win-67694[8] or IDN-7568[9]), or heterocyclic derivatives (PTP[10]).

The first reported study of ligands projecting into the prime side looked at the effect of methylene spacers on the binding of a phenyl group.[11] The authors identified the peptidomimetic AcYVAD$(CH_2)_5$Ph, **1**, as a potent ICE inhibitor (K_i = 18.5 nM). Later, our group[12] reported sulfonamide derivatives having the potential for intramolecular H-bonding effects that were able to rigidify the backbone. Our analog **2** exhibited comparable potency (K_i = 4 nM) to **1**. These appear to be the only reports directed at fully accessing the prime side binding pocket. From analysis of the X-ray crystal structure of ICE and consistent with the observed SAR, it is evident that the prime side pocket is hydrophobic in nature, since it is surrounded by hydrophobic amino acid residues (Ile176, Pro177, and Ile239).

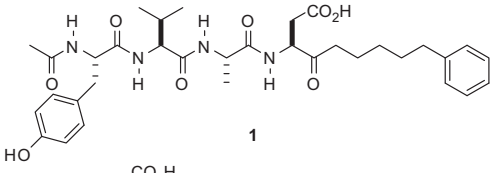

1

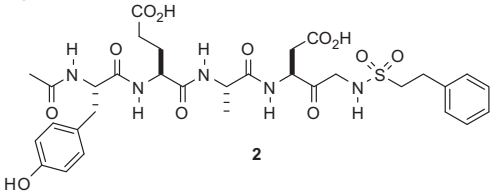

2

While providing valuable information related to the prime side interactions, these reports left a great deal of questions unanswered. We wished to fill this knowledge gap in order to better design ICE inhibitors. To rapidly assess prime side SAR, a strategy of optimizing this fragment on a truncated P side moiety was envisioned. This was accomplished by utilizing a carbobenzyloxy aspar-

* Corresponding author. Address: MS 8220-4225, Pfizer Global R&D, Eastern Point Road, Groton, CT 06340, United States. Tel.: +1 860 686 9379.
E-mail address: paul.galatsis@pfizer.com (P. Galatsis).

0960-894X/$ - see front matter © 2010 Elsevier Ltd. All rights reserved.
doi:10.1016/j.bmcl.2010.07.031

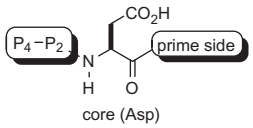

Figure 1. General structural features of an ICE inhibitor.

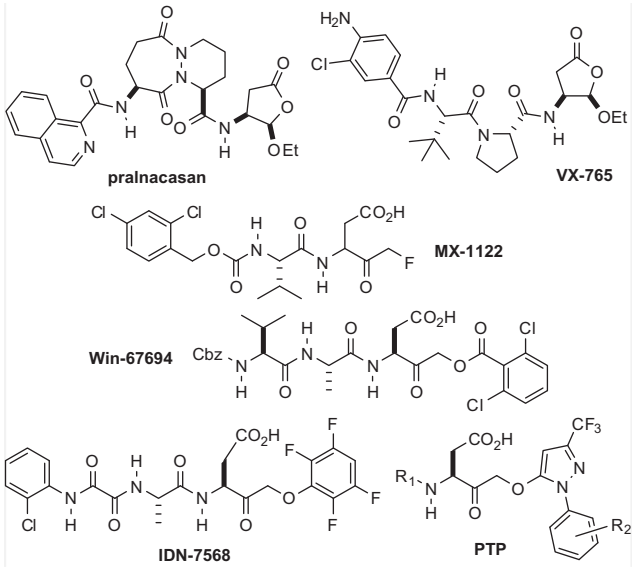

Figure 2. Representative ICE inhibitors illustrating the typical structural motifs found on the prime side.

tic acid core to construct a series of acyloxyalkyl and amidooxyalkyl ketones. The advantage of using this single amino acid substrate was that it increased the ease of synthesis and simplified the analysis of the final products since, for example, di- and tripeptide acyloxyalkyl ketones can lead to bimodal inhibitors.[13] This strategic approach was completed by appending the optimized prime side fragment to the full length P side to afford ICE inhibitors with improved potency.

Synthesis of the aspartyl acyloxyalkyl ketones **4** followed the protocol outlined in Scheme 1.[14] The known[15] bromoketone **3** could be converted into the desired esters **4** by bromide displacement with the corresponding carboxylic acid followed by deprotection of the aspartyl β-acid with TFA. Esters **4** were tested as inhibitors of ICE using a recombinant form of the enzyme and monitored by fluorescence (Table 1).[13] Ketone **5** was synthesized, based on our strategic design, as a reference standard to be analogous with **1**.

With compounds **4** in-hand, it was quickly observed that simple acyloxyalkyl ketones, such as **4a**, demonstrated improved activity (14-fold) compared to **5**. Phenylalkyl derivatives **4b** and **4c** probe the depth of the prime side pocket and showed optimal binding with two methylene spacers. The tolerability of heteroatoms in the linker was examined with compounds **4d–f**. While a nitrogen atom (**4f**) is tolerated, oxygen (**4d**) and sulfur (**4e**) show a modest

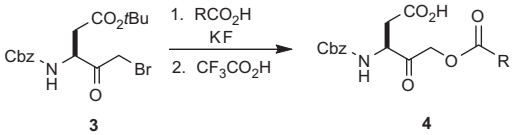

Scheme 1. Preparation of aspartyl acyloxyalkyl ketones.

Table 1
Comparison of binding affinity for select compounds[a]

Entry	Compound	K_i (μM)
5	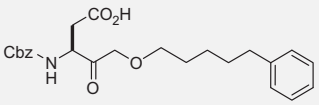	119
4a	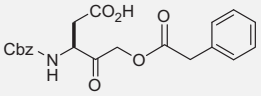	8.3
4b	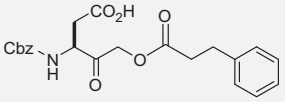	4.5
4c	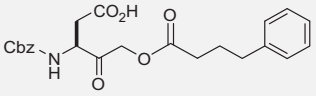	16
4d	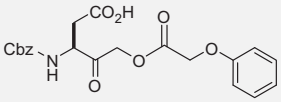	1.7
4e	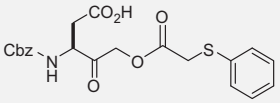	1.1
4f	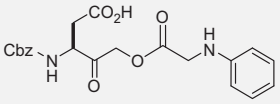	5.6
4g	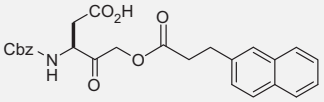	6.0
4h	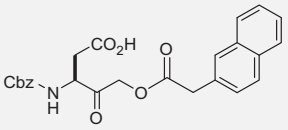	1.3
4i	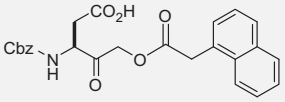	0.5
4j	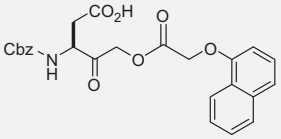	1.0
4k	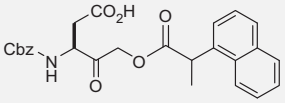	1.0
4l	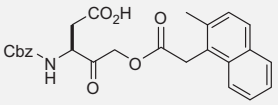	4.4
4m	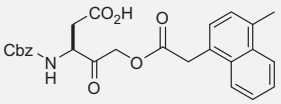	1.3
4n	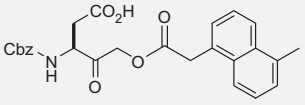	2.0
4o	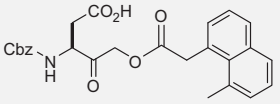	8.5

Table 1 (*continued*)

Entry	Compound	K_i (μM)
4p	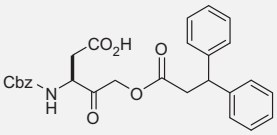	0.8
4q	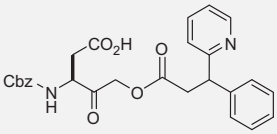	1.1
4r	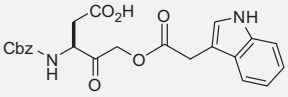	0.6
4s	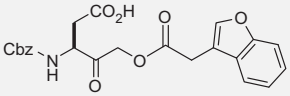	0.8
4t	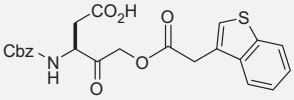	1.2
4u	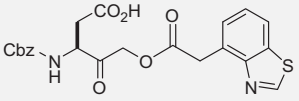	2.6

[a] For a description of the assay see Ref. 13. K_i values are the geometric mean of two or more experiments.

2.6- and 4-fold, respectively, improvement in binding relative to **4b**. A 2-naphthyl moiety (**4g**) modification of **4b** shows the additional phenyl was tolerated. However, a 4.6-fold improvement in binding was observed by shortening the chain by a single methylene group (**4h**). Compound **4i** maintains the shorter linker but now changes the orientation of the naphthyl moiety by linking through the 1-position. This modification provided a 12-fold increase in potency relative to **4g**. Inserting an oxygen atom into the linker, as in **4j**, was tolerated with only a slight twofold decrease in potency relative to **4i**. In an attempt to restrict the conformational space the naphthyl fragment could occupy, the methylene spacer in **4i** was methylated to afford **4k**, which was equipotent with **4j**. While multiple compounds were prepared, compounds **4l–o** summarizes the naphthyl moiety substituent effects. Substitution at the 4-position (**4m**) and 5-position (**4n**) were better tolerated than at the 2-position (**4l**) or 8-position (**4o**). Adding a phenyl substituent to the linker chain of **4b** generated **4p** that proved to be equipotent to **4i**. Compound **4q** is the result of addition of a pyridyl fragment to linker of **4b**. This resulted in a slight erosion of potency compared to **4i**. Compounds **4r–u** provided additional examples that showed the prime side could tolerate additional polarity. The indole moiety of **4r** proved to be the most potent, followed by benzofuran **4s**, benzothiophene **4t**, and benzothiazole **4u**.

These results strongly suggest that the principal feature needed for optimal activity of the prime side ester is the juxtaposition of the aryl group within the ICE prime side pocket. In order to study this prime side interaction more fully, we obtained X-ray crystal structures of **4i**. This juxtaposition is displayed in Figure 3, which shows the binding pose of **1** relative to ester **4i**. The Asp β-carboxy binds into the oxy-anion hole. The Cbz group of **4i** reaches into the S2 pocket, whereas **1** extends to fully interact with the P side. On the prime side, the phenyl group of **1** and the naphthyl ring of **4i** occupy very similar positions in the hydrophobic pocket. This was accomplished by the linker taking similar trajectories. More

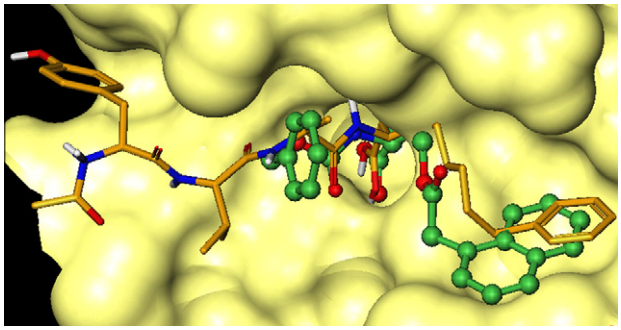

Figure 3. X-ray structure of **1** (orange) and **4i** (green) in ICE active site.

specifically, the naphthyl group binds in the hydrophobic region formed by the Ile176, Pro177, and Ile239 side chains. The naphthyl group is oriented with its second phenyl ring binding edge-wise towards Gly238 which is located in a beta strand.

Interestingly, the potent diphenyl derivative **4p** docked with its ester group oriented essentially 90° to the ester group of **4i** (Fig. 4). One prime side phenyl ring of **4p** intersects almost perpendicularly to the second ring of the naphthyl group in **4i**, but still formed hydrophobic contacts with Ile176 and Ile239. The second phenyl group in **4p** orients proximal to the Asp288 loop in the C-terminus region of the p20 domain. Since this second phenyl group resulted in more than a sevenfold enhancement in potency, relative to **4b**, this intriguing binding pose highlights an additional binding subsite that could be targeted by prime side groups.

Complementary to these studies and as part of our ICE inhibitor project, a diverse combinatorial library was generated to fully explore the chemical space associated with the prime side pocket of the protease active site. From this array, hydroxamic acid derivative **6** was determined to be an active compound. This hit was selected for further optimization to probe the nature of the hydrophobic pocket and explore the effect of the hydroxamic acid functional group on ICE inhibition. Could the hydroxamate functional group be isosteric with the ester group in this series of ICE inhibitors?

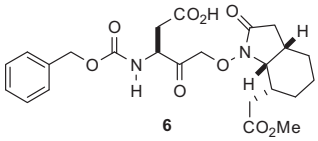

6

In order to determine which attributes of this compound imparted it with such potency, an X-ray crystal structure of **6** bound in the active site of the enzyme was determined (Fig. 5). Analysis of the

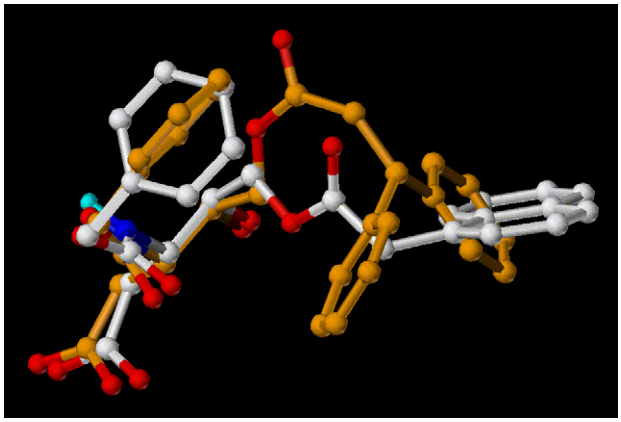

Figure 4. Docked overlay of **4i** (white) and **4p** (orange).

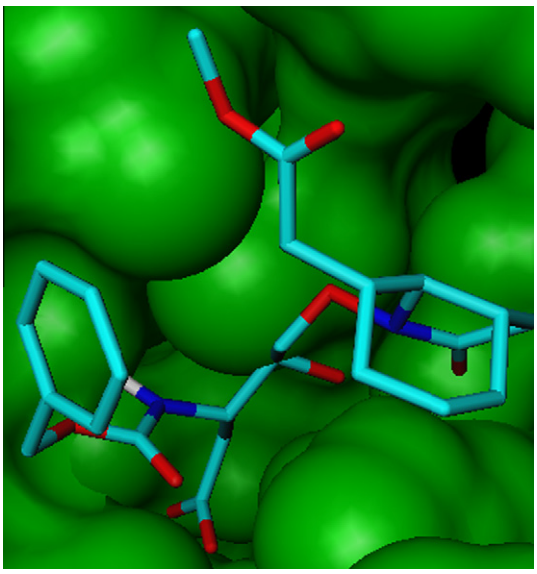

Figure 5. X-ray binding pose for **6**.

structural data indicated that **6** made interactions, with respect to the P1 position, as seen with other inhibitors. That is, the β-carboxyl Asp group was bound to the oxy-anion hole formed by the Arg341, Arg179, and Gln283 residues. Additional interactions observed were the carbonyl of the Asp moiety H-bonding with His237 and the amide nitrogen H-bonding to the backbone Ser339 carbonyl. A unique feature of **6**, captured by this structure, is the additional H-bond with Gly238 residue from the carbonyl of the hydroxamic acid moiety. The crystal structure also revealed that the carbomethoxy of the hydroxamic acid moiety was able to reach and presumably make contacts in the S2 pocket, along with the Cbz protecting group (Fig. 5).

Having made a preliminary attempt to rationalize which structural features of the hydroxamic acid moiety were utilized for its binding, the next step was to vary these groups to gain greater insight into these interactions. Hydroxamates **7** implement the same strategy used to examine the ester SAR. These inhibitors maintained the truncated core fragment and the prime side moiety was optimized for potency.

The hydroxamates **7** could be synthesized[14] in a straightforward manner (Scheme 2) from the readily available aspartic acid derivative **3**[15] using a variation of the chemistry that was employed in the preparation of the esters **4**. Displacement of the bromide now by appropriately substituted hydroxamic acids, followed by deprotection with TFA afforded the desired target compounds **7**.

The series of compounds **7** were assayed for ICE inhibitory activity and the results are summarized in Table 2. In addition to **6**, compound **5** reprised its role as a reference compound as a way to calibrate our strategic approach and relate these compounds with esters **4**. Thus, compound **6** was found to be eightfold more potent

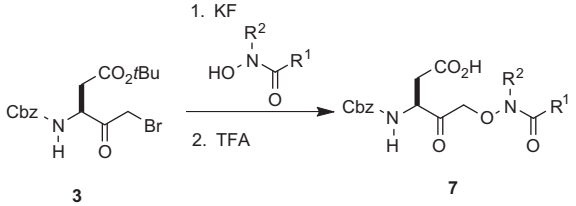

Scheme 2. Preparation of aspartyl amidooxyalkyl ketones.

Table 2
ICE enzyme inhibition data[a]

Entry	Structure	K_i (μM)
5	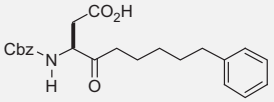	119
6	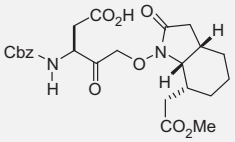	15.0
7a	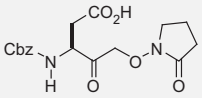	87.2
7b	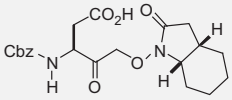	9.20
7c	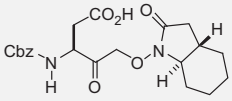	17.5
7d	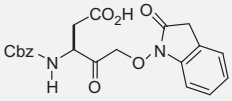	6.77
7e	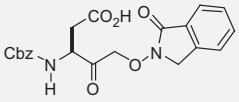	14.0
7f	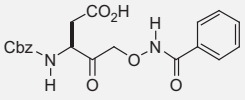	21.0
7g	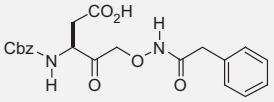	66.5
7h	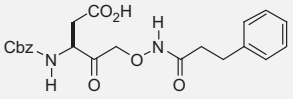	27.5
7i	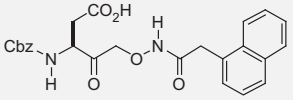	84.0
7j	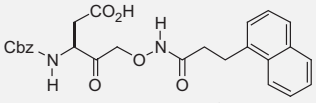	298
7k	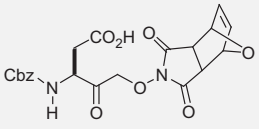	1.50

[a] For a full description of the assays see Ref. 8. Values are the geometric mean of two or more experiments.

than **5**. Compound **7a** contains a minimally functionalized hydroxamate fragment which proved to be 5.8-fold less potent than **6** but equipotent with **5**. Thus, the hydroxamate functional group was making more productive interactions when compared to **5** and different from those with **4**. Compounds **7b** and **7c** provide some insight into the substituents required for improved binding interactions. These two compounds lack the pendant carbomethoxy group found in **6** but exhibited approximately equivalent potency.

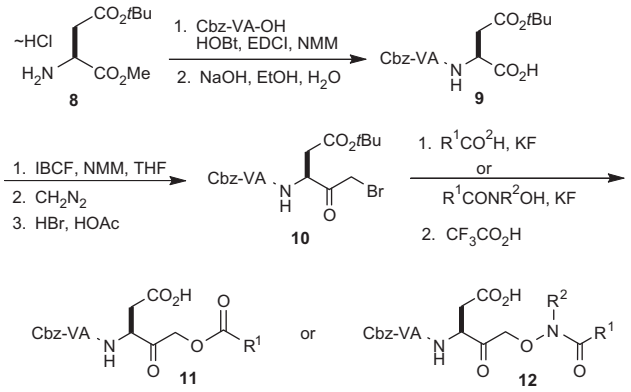

Scheme 3. Preparation of tripeptide acyloxyalkyl ketones.

Clearly, the carbomethoxy group was not contributing in a productive manner, to the binding interactions, thus giving rise to the observed results. No increases in potency were observed with **7d** and **7e** as the six-membered ring was made aromatic. Compounds **7f–j** were designed to probe the hydrophobic characteristics of the prime side region. Implementation of these moieties on the ester variation proved to be a very successful approach for achieving greater potency but this SAR did not translate to the hydroxamic acid variation. Indeed, on the contrary, potency was negatively impacted. Interestingly, improvements to potency (80-fold relative to **1**) were recovered with the oxa[2.2.1]bicyclo **7k**. Presumably, the convex nature of this group fills the hydrophobic pocket more effectively.

Having identified prime side fragments that greatly increased binding efficiency relative to the reference compound **5**, the time to close the loop on the validation of our strategy arrived. Several of the optimized prime side groups with demonstrated potency improvements were combined with peptide P side fragments to generate fully derivatized ICE inhibitors that were then evaluated for overall improvement of binding efficacy. The commercially available, orthogonally protected aspartic acid derivative **8** was transformed using robust chemistry into the desired prime side analogs **11** and **12** (Scheme 3).[14] Elongation of **8** using standard peptide chemistry afforded the Cbz-capped tripeptide acid **9** which was converted to the corresponding bromoketone **10**. Deprotection

Table 3
Comparison of in vitro[a] and whole cell[b] inhibitory potency

Entry	Structure	K_i (μM)	IC_{50} (μM)	PBMC (μM)
1	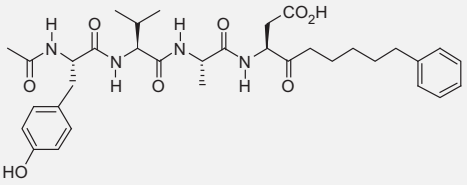	0.011	0.078	0.9
13	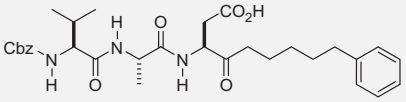	0.134	0.976	4.9
11a	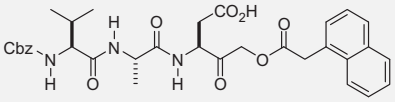	0.003[c]	0.002	0.6
11b	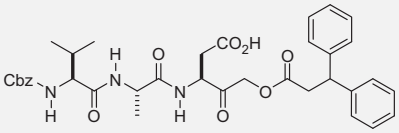	0.001[c]	0.005	4.3
11c	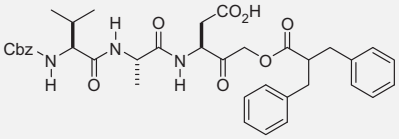	0.002[c]	0.003	1.4
12a	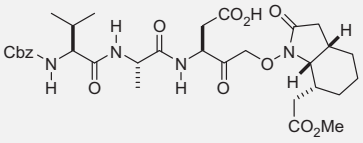	0.007	0.026	4.8
12b	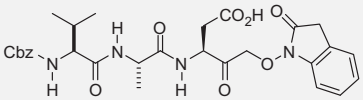	0.002	0.003	3.0
12c	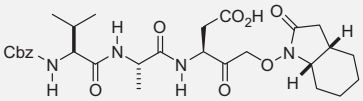	0.001	0.003	2.4

[a] For a description of the assay see Ref. 13. K_i values are the geometric mean of two or more experiments.
[b] For a description of the assay see Ref. 16.
[c] Mechanistic change to irreversible inhibition (bimodal kinetics).

of the Asp β-carboxylic acid followed bromide displacement with the appropriate carboxylic or hydroxamic acid (vide supra) to generate the desired targets **11** and **12**.

With these compounds in-hand, their potency for ICE inhibition was determined and the data is presented in Table 3. Compound **13** shows that the P4 substituent of **1** is more efficient at binding compared to the Cbz group present in **12**. The ester analogs **11** and hydroxamates **12** are significantly more potent than the reference compound **13**. The analysis for these inhibitors was complicated by the observation that these more potent peptide derivatives of esters **11** could now serve as leaving groups. This mechanistic switch is not unknown, since di- and tripeptide acyloxyalkyl ketones can lead to bimodal inhibitors as previously described.[13]

Comparison of these compounds in a functional assay using human peripheral blood mononuclear cells (PBMC) shows a much different result. In this functional assay, esters **11b** and **11c** are approximately equipotent with reference compound **13**. In contrast **11a** is about 10-fold more potent in the PBMC assay than the other compounds. This poor correlation between enzymatic inhibition and cell-based activity has been noted previously[4a] and is problematic for the prediction and discovery of an ICE inhibitor with therapeutic potential. Since ICE is an intracellular enzyme, the loss of activity in going from the enzyme assay to the cell-based assay may, in part, be a result of transport problems across the cellular membrane. This explanation, however, seems far too simplistic when structurally similar compounds such as **11a** and **11b** show divergent functional activity. A satisfactory explanation of this poor correlation awaits future study.

Having examined the inhibitory activity of the esters **11**, our focus was directed towards the hydroxamic acid terminated peptidomimetics **12** (Table 3). Compound **12a**, based on the original library hit **6**, was found to be almost 40-fold more potent, by IC_{50}, than reference compound **13**. Of the three hydroxamates presented in Table 3, **12a** proved to be the weakest. Compounds **12b** and **12c** were found to be about eightfold more potent. Additionally, hydroxamates **12** stand in contrast to esters **11**. The former did not display the change in mechanism, from reversible to irreversible enzyme inhibition, observed with the later despite them both having comparable potency.

In summary, we have designed and synthesized a series of ICE inhibitors with a variety of esters and hydroxamates that interact with the prime side amino acid residues of the enzyme. These inhibitors were designed and optimized using a protected aspartic acid core and then the most potent groups were appended to a larger tripeptide producing low nanomolar ICE inhibitors. The results demonstrate that, while potent inhibitors can be generated, one must be cognizant of the nature of the binding interaction. This is important to ensure the mechanism of inhibition does not change. In sharp contrast to the ester variation, the hydroxamates appear to have a narrower SAR trend. These two series have resulted in an improved understanding of the binding requirements of the lipophilic pocket on the prime side of the enzyme and this information can now be utilized in the design of future ICE inhibitors.

Supplementary data

Supplementary data (coordinate files (pdb) containing the active site residues with the bound ligand for Figs. 3 and 5) associated with this article can be found, in the online version, at doi:10.1016/j.bmcl.2010.07.031.

References and notes

1. (a) Thornberry, N. A.; Bull, H. G.; Calaycay, J. R.; Chapman, K. T.; Howard, A. D.; Kostura, M. J.; Miller, D. K.; Molineaux, S. M.; Weidner, J. R.; Aunin, J.; Elliston, K. O.; Ayala, J. M.; Casano, F. J.; Chin, J.; Ding, G. J.-F.; Egger, L. A.; Gaffney, E. P.; Limjuco, G.; Palyha, O. C.; Raju, S. M.; Rolando, A. M.; Salley, J. P.; Yamin, T.-T.; Lee, T. D.; Shively, J. E.; MacCross, M.; Mumford, R. A.; Schmidt, J. A.; Tocci, M. J. *Nature* **1992**, *356*, 768; (b) Thornberry, N. A. *Br. Med. Bull.* **1996**, *53*, 478; (c) Bird, S.; Zou, J.; Wang, T.; Munday, B.; Cunningham, C.; Secombers, C. J. *Cytokine Growth Factor Rev.* **2002**, *13*, 483; (d) Joosten, L. A. B.; van den Berg, W. B. *Drug Discov. Today* **2006**, *3*, 169.
2. (a) Ator, M. A.; Dolle, R. E. *Curr. Pharm. Des.* **1995**, *1*, 191; (b) Giegel, D. A.; Kostlan, C. R. *Annu. Rep. Med. Chem.* **1998**, *33*, 183; (c) Talanian, R. V.; Brady, K. D.; Cryns, V. L. *J. Med. Chem.* **2000**, *43*, 3351; (d) Ashwell, S. *Expert Opin. Ther. Patents* **2001**, *11*, 1593; (e) Randle, J. C. R.; Harding, M. W. H.; Ku, G.; Schonharting, M.; Kurrle, R. *Expert Opin. Investig. Drugs* **2001**, *10*, 1207; (f) Braddock, M.; Quinn, A. *Nat. Rev. Drug Discov.* **2004**, *3*, 1; (g) Dinarello, C. A. *Curr. Opin. Pharmacol.* **2004**, *4*, 378; (h) Le, G. T. E.; Abbenante, G. *Curr. Med. Chem.* **2005**, *12*, 2963; (i) Fischer, U.; Schulze-Osthoff, K. *Pharmacol. Rev.* **2005**, *57*, 187.
3. (a) Wilson, K. P.; Black, J. F.; Thomson, J. A.; Kim, E. E.; Griffith, J. P.; Navia, M. A.; Murcko, M. A.; Chambers, S. P.; Aldape, J. P.; Raybuck, S. A.; Livingston, D. J. *Nature* **1994**, *370*, 270; (b) Walker, N. P. C.; Talanian, R. V.; Brady, K. D.; Dang, L. C.; Bump, N. J.; Ferenz, C. R.; Franklin, S.; Ghayur, T.; Hackett, M. C.; Hammill, L. D.; Herzog, L.; Hugunin, M.; Houy, W.; Mankovick, J. A.; McGuiness, L.; Orlewicz, E.; Paskind, M.; Pratt, C. A.; Reis, P.; Summani, A.; Terranova, M.; Welch, J. P.; Moller, A.; Tracey, D. E.; Kamen, R.; Wong, W. W. *Cell* **1994**, *78*, 343.
4. (a) Thornberry, N. A.; Molineaux, S. M. *Protein Sci.* **1994**, *4*, 3; (b) Rano, T. A.; Timkey, T.; Peterson, E. P.; Rotonda, J.; Nicholson, D. W.; Becker, J. W.; Champman, K. T.; Thornberry, N. A. *Chem. Biol.* **1997**, *4*, 149.
5. (a) Rudolphi, K.; Gerwin, N.; Verzijl, N.; van der Kraan, P.; van den Berg, W. *Osteoarthritis Cartilage* **2003**, *11*, 738; (b) Bauer, C.; Loher, F.; Dauer, M.; Mayer, C.; Lehr, H. A.; Schonharting, M.; Hallwachs, R.; Endres, S.; Eigler, A. *Dig. Dis. Sci.* **2007**, *52*, 1642.
6. Wannamaker, W.; Davies, R.; Namchuk, M.; Pollard, J.; Ford, P.; Ku, G.; Decker, C.; Charifson, P.; Weber, P.; Germann, U. A.; Kuida, K.; Randle, J. C. R. *J. Pharmacol. Exp. Ther.* **2007**, *321*, 509.
7. Cai, S. X.; Guan, L.; Jia, S.; Wang, Y.; Yang, W.; Tseng, B.; Drewe, J. *Bioorg. Med. Chem. Lett.* **2004**, *14*, 5295.
8. Miller, B. E.; Krasney, P. A.; Gauvin, D. M.; Holbrook, K. B.; Koonz, D. J.; Abruzzese, R. V.; Miller, R. E.; Pagani, K. A.; Dolle, R. E.; Ator, M. A.; Gilman, S. C. *J. Immunol.* **1995**, *154*, 1331.
9. Ueno, H.; Kawai, M.; Shimokawa, H.; Hirota, M.; Ohmi, M.; Sudo, R.; Ohta, A.; Arano, Y.; Hattori, K.; Ohmi, T.; Kato, N.; Kojima, M.; Ueno, Y.; Yamamoto, M.; Moriguchi, Y.; Eda, H.; Masubuchi, K. *Bioorg. Med. Chem. Lett.* **2009**, *19*, 199.
10. Kulkarni, S. S.; Kulkarni, V. M. *J. Med. Chem.* **1999**, *42*, 373.
11. Mjalli, A. M. M.; Chapman, K. T.; MacCross, M.; Thornberry, N. A. *Bioorg. Med. Chem. Lett.* **1993**, *3*, 2689.
12. Harter, W. G.; Albrecht, H.; Brady, K.; Caprathe, B.; Dunbar, J.; Gilmore, J.; Hays, S.; Kostlan, K. R.; Lunney, B.; Walker, N. *Bioorg. Med. Chem. Lett.* **2004**, *14*, 809.
13. Brady, K. D. *Biochemistry* **1998**, *37*, 8508.
14. All compounds were characterized by ^{1}H NMR, MS and were >98% pure by either CHN analysis or analytical HPLC.
15. Albeck, A.; Estreicher, G. *Tetrahedron* **1997**, *53*, 5325.
16. Human peripheral blood mononuclear cells (PBMC) were isolated from heparinized blood by centrifugation over a Ficoll cushion and then washed three times with PBS. The PBMC's were suspended in a medium containing RPMI 1640 with glutamine, penicillin, streptomycin, and 2% human AB serum and then plated at 106 cells per well in a 96 well flat bottom plate. PBMC's were stimulated overnight with 10 ng/mL of LPS in the presence or absence of inhibitor. The medium was harvested and the level of mature IL-1β was determined using an ELISA kit from R&D Systems. Compound inhibition (IC_{50} values) was assessed by determining the concentration of agent which reduced IL-1β levels by 50%.